Published July 11, 2011

Epithelial transglutaminase 2 is needed for T cell interleukin-17 production and subsequent pulmonary inflammation and fibrosis in bleomycin-treated mice

Keunhee Oh,[1] Hyung-Bae Park,[1] Ok-Jin Byoun,[1] Dong-Myung Shin,[2] Eui Man Jeong,[2] Young Whan Kim,[3] Yon Su Kim,[4] Gerry Melino,[5] In-Gyu Kim,[2] and Dong-Sup Lee[1]

[1]Laboratory of Immunology, Department of Biomedical Sciences / Transplantation Research Institute, [2]Department of Biochemistry and Molecular Biology, [3]Division of Pulmonary and Critical Care Medicine, [4]Department of Internal Medicine, Seoul National University College of Medicine, Seoul 110-799, Korea
[5]MRC Toxicology Unit, University of Leicester, Leicester LE1 9HN, England, UK

Pulmonary fibrosis is a potentially life-threatening disease that may be caused by overt or asymptomatic inflammatory responses. However, the precise mechanisms by which tissue injury is translated into inflammation and consequent fibrosis remain to be established. Here, we show that in a lung injury model, bleomycin induced the secretion of IL-6 by epithelial cells in a transglutaminase 2 (TG2)–dependent manner. This response represents a key step in the differentiation of IL-17–producing T cells and subsequent inflammatory amplification in the lung. The essential role of epithelial cells, but not inflammatory cells, TG2 was confirmed in bone marrow chimeras; chimeras made in TG2-deficient recipients showed reduced inflammation and fibrosis, compared with those in wild-type mice, regardless of the bone marrow cell phenotype. Epithelial TG2 thus appears to be a critical inducer of inflammation after noninfectious pulmonary injury. We further demonstrated that fibroblast-derived TG2, acting downstream of transforming growth factor-β, is also important in the effector phase of fibrogenesis. Therefore, TG2 represents an interesting potential target for therapeutic intervention.

CORRESPONDENCE
Dong-Sup Lee:
dlee5522@snu.ac.kr
In-Gyu Kim:
igkim@plaza.snu.ac.kr

Abbreviations used: B6, C57BL/6; BALF, bronchoalveolar lavage fluid; BLM, bleomycin; CyM, cysteamine; ECM, extracellular matrix; IPF, idiopathic pulmonary fibrosis; pro-SP-C, pro-surfactant protein-C; MLEC, mouse lung epithelial cell; MLF, mouse lung fibroblast; TG2, transglutaminase 2.

Fibroproliferative diseases, including pulmonary fibrosis, liver cirrhosis, and cardiovascular and renal fibrosis, are caused by chronic inflammation subsequent to persistent tissue damage (Wynn, 2007). Unlike liver cirrhosis, which, in many developing countries frequently follows chronic infection with hepatitis B or C virus, pulmonary fibrosis, and particularly idiopathic pulmonary fibrosis (IPF)—the most frequent and devastating form of the disease—typically follows noninfectious (i.e., physicochemical) tissue injury (Rogliani et al., 2008).

Epithelial cells have recently been shown to play critical roles in the initiation and perpetuation of inflammation and fibrosis (Hardie et al., 2009). Specifically, altered repair triggered by epithelial injury has been suggested to contribute to the pathogenesis of IPF (Rogliani et al., 2008). Thus, the roles of pulmonary epithelial cells in the inflammatory cascades activated after noninfectious injury, and the key signaling mediators of this process, are now being actively investigated.

The Th17 response was originally described as providing protective immunity against pulmonary infection (Aujla et al., 2007; Korn et al., 2009). The recent identification of TGF-β and IL-6/IL-1 as cytokines that promote Th17 differentiation, IL-23 as a signal for Th17 cell survival and effector function, and RORγt and RORα as Th17 lineage-specific transcription factors (Weaver et al., 2007; McGeachy and Cua, 2008; Korn et al., 2009) confirmed the identity of Th17 cells as a distinct inflammatory T helper cell subset. Th17 cells participate in the initial

© 2011 Oh et al. This article is distributed under the terms of an Attribution–Noncommercial–Share Alike–No Mirror Sites license for the first six months after the publication date (see http://www.rupress.org/terms). After six months it is available under a Creative Commons License (Attribution–Noncommercial–Share Alike 3.0 Unported license, as described at http://creativecommons.org/licenses/by-nc-sa/3.0/).

The Rockefeller University Press $30.00
J. Exp. Med. Vol. 208 No. 8 1707-1719
www.jem.org/cgi/doi/10.1084/jem.20101457

Supplemental Material can be found at:
http://jem.rupress.org/content/suppl/2011/07/10/jem.20101457.DC1.html

The Journal of Experimental Medicine

Published July 11, 2011

inflammatory cascades that are activated after acute lung damage and that lead to permanent tissue damage in asthma and chronic obstructive pulmonary disease (Traves and Donnelly, 2008). It further appears that the Th17 response may play an important role in the amplification of the inflammatory response after noninfectious pulmonary injury (Lo Re et al., 2010; Sonnenberg et al., 2010; Wilson et al., 2010). However, the factors that induce Th17 responses after noninfectious tissue damage in vivo remain to be identified.

Transglutaminase 2 (TG2) is a calcium-dependent enzyme that catalyzes the cross-linking of proteins (Lorand and Graham, 2003). Irreversible cross-linking of extracellular matrix (ECM) proteins by secreted transglutaminase is important in promoting the net accumulation of ECM molecules (Verderio et al., 2004). Elsewhere, the essential role of TG2 in hepatic and renal fibrosis during the effector phase of fibrogenesis has been confirmed (Shweke et al., 2008; Elli et al., 2009).

A potential role for TG2 in inflammation has also recently been highlighted. As TG2 is induced by various physical, chemical, and biological stresses (Ientile et al., 2007) and, in turn, activates NF-κB signaling by stimulating the polymerization of IκB (Park et al., 2006), it may link tissue injury and inflammatory responses. Recently, we showed that activation of TG2 in epithelial cancer cells induces IL-6 production, resulting in enhanced tumor progression (unpublished data). Because TG2 has also been implicated in TGF-β activation (Kojima et al., 1993), it may activate both TGF-β and inflammatory signals (including those induced by IL-6), leading to Th17 differentiation. Moreover, dysregulated activation of TG2 has been observed in various human inflammatory diseases, including newly defined Th17-mediated diseases (Kim, 2006). On this basis, we suggest that TG2, in conjunction with Th17 cells, may provide the fundamental link between tissue injury and inflammation.

In this study, we used bleomycin (BLM)-induced pulmonary fibrosis as an experimental model of human IPF. Using bone marrow chimeric mice generated from WT and TG2-null mice, we demonstrate two important points: first, that epithelial cells are critical in the initiation and perpetuation of the inflammation that leads to fibrosis, and second, that epithelial TG2 activity after noninfectious injury is essential for inducing IL-6 production, which, in turn, triggers Th17-mediated

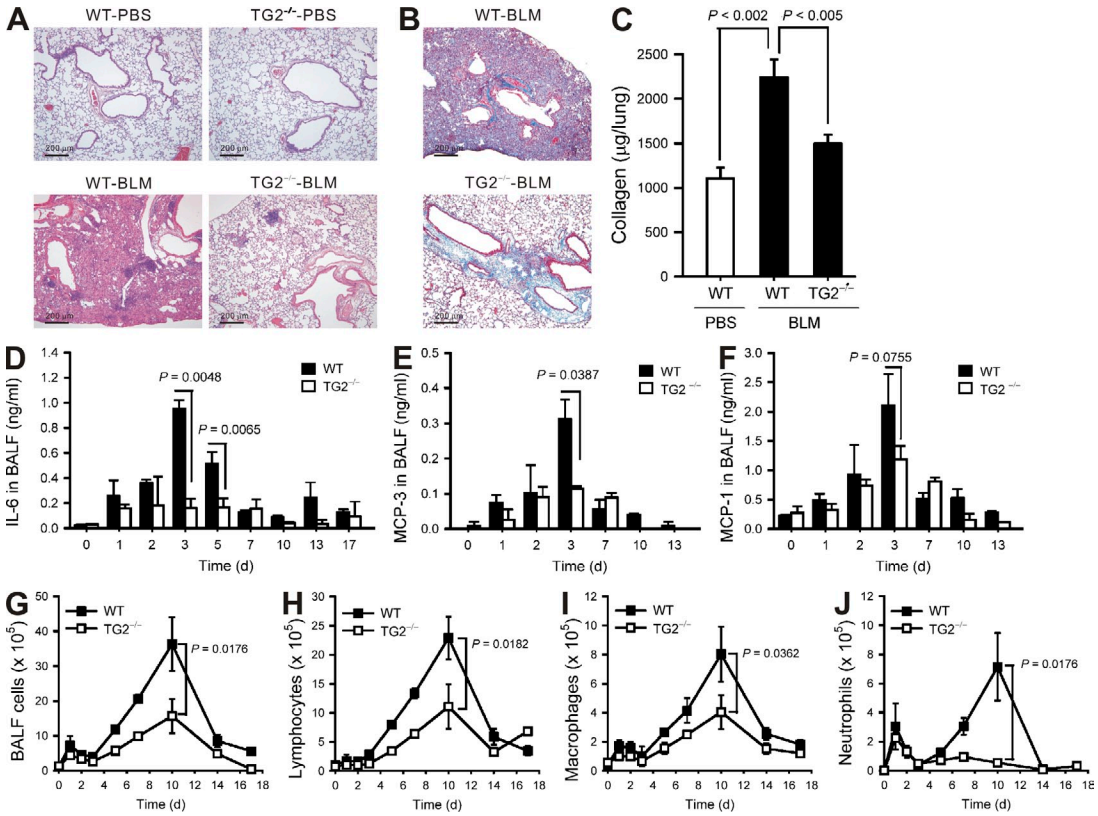

Figure 1. TG2 deficiency reduces BLM-induced pulmonary inflammation and fibrosis. (A–C) Representative photographs of lungs from WT and TG2$^{-/-}$ mice 21 d after intratracheal instillation of BLM (1.5 mg/kg) or PBS. Sections were stained with H&E (A) or Masson-trichrome (B). Pulmonary collagen content of the lungs was determined by the Sircol assay (C). (D–F) Levels of IL-6 (D), MCP-1 (E), and MCP-3 (F) in BALF of WT and TG2$^{-/-}$ mice after BLM-exposure were determined by ELISA. (G–J) Inflammatory cells in BALF from WT B6 and TG2$^{-/-}$ mice. BLM-exposed mice were sacrificed to harvest BALF on the indicated days. Numbers of total cells (G), lymphocytes (H), macrophages (I), and neutrophils (J) in BALF were determined by flow cytometric analysis. Data represent means ± SD of three independent determinations with BALF or lung tissues, and $n = 5$ (A–C) or $n = 3$ mice/group for each time point (D–J).

Published July 11, 2011

inflammatory amplification in the lung. Moreover, we separately showed that the activation of TG2 in fibroblasts (downstream of TGF-β) is important during the effector phase of fibrogenesis. TG2 may therefore represent a useful therapeutic target.

RESULTS

TG2 mediates inflammatory cell recruitment and fibrosis in the BLM-treated lung

To explore the role of TG2 in the inflammation and fibrosis caused by noninfectious lung injury, we used a mouse BLM-induced pulmonary fibrosis model. WT C57BL/6 (B6) and $TG2^{-/-}$ mice were exposed to BLM by intratracheal instillation and sacrificed 21 d later. Histopathological examination of the lungs of BLM-treated $TG2^{-/-}$ mice revealed markedly reduced inflammatory cell infiltration (Fig. 1 A) and collagen deposition (Fig. 1 B) compared with WT animals. A Sircol assay revealed significantly decreased total lung collagen content in BLM-treated $TG2^{-/-}$ mice compared with WT controls (Fig. 1 C). To evaluate the factors responsible for initiating pulmonary inflammation, we measured the levels of cytokines and chemokines in bronchoalveolar lavage fluid (BALF). Notably, IL-6 was detected (by ELISA) in BALF from WT mice, but not from $TG2^{-/-}$ mice, 3 d after BLM treatment (Fig. 1 D). BALF levels of both MCP-1 and MCP-3 were higher in WT mice compared with $TG2^{-/-}$ animals (Fig. 1, E and F). Semiquantitative RT-PCR analyses further showed that BLM treatment significantly increased the expression of key cytokines and chemokines on day 3 in the lungs of WT mice, but not in $TG2^{-/-}$ mice (Fig. S1). Increased production of cytokines and chemokines in WT mice compared with $TG2^{-/-}$ mice were mirrored in the inflammatory cell recruitment in BALF. Flow cytometric analysis of the cells present in BALF revealed that BLM-treated WT mice exhibited gradual increases in the numbers of total inflammatory cells (Fig. 1 G), lymphocytes (Fig. 1 H), macrophages (Fig. 1 I), and neutrophils (Fig. 1 J) over a 10-d period, whereas significantly fewer cells were recruited to the lungs of the $TG2^{-/-}$ mice (Fig. 1, G–J). Although the initial recruitment of neutrophils 1 d after BLM instillation was comparable in WT and $TG2^{-/-}$ mice (Fig. 1 J), secondary neutrophilic infiltration was observed only in the WT mice (Fig. 1 J).

TG2-mediated IL-6 production triggers a Th17 response after BLM-induced lung injury

IL-6 is a key stimulator of Th17 cell differentiation (Weaver et al., 2007; McGeachy and Cua, 2008; Korn et al., 2009), and the role of Th17 cells in the immune response that follows pulmonary infection is well established (Aujla et al., 2007; Korn et al., 2009). We tested whether TG2-mediated IL-6 secretion contributed to Th17 differentiation in lungs damaged by noninfectious injury (caused by BLM treatment). Numbers of $CD4^+$ T cells in BALF, which constitute 40–70% of the total BALF T cell population, increased at days 5, 7, and 10 (unpublished data). WT mice displayed ~6-fold higher percentages and numbers of $CD4^+$ $IL\text{-}17^+$ T cells (hereafter

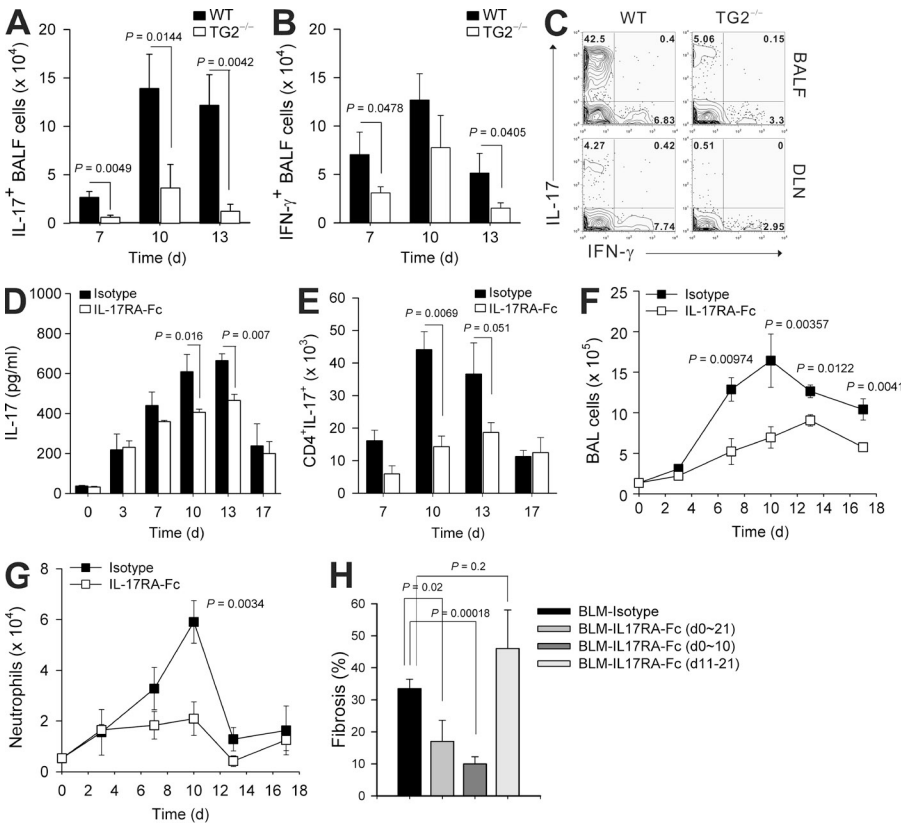

Figure 2. BLM-mediated pulmonary injury triggers a Th17 response. WT B6 and $TG2^{-/-}$ mice received an intratracheal instillation of BLM (1.5 mg/kg) and were sacrificed to harvest BALF on the indicated days. Cells from BALF were stimulated with PMA and ionomycin and intracellular cytokines were detected by flow cytometric analysis. (A and B) Numbers of $CD4^+$ cells producing IL-17 (A) or IFN-γ (B) in BALF of BLM-exposed WT B6 and $TG2^{-/-}$ mice. (C) The percentages of $CD4^+$ cells producing IL-17 or IFN-γ in BALF and draining lymph nodes (DLN) of WT B6 and $TG2^{-/-}$ mice were determined by flow cytometric analysis 10 d after BLM exposure. Dot plots are gated on $CD4^+$ T cells. (D–H) BLM-exposed WT B6 mice were treated with IL-17RA-Fc or isotype control for 10 d (100 μg/mouse/day, i.p.). IL-17 levels (D) and the numbers of $CD4^+IL\text{-}17^+$ cells (E), total cells (F), and neutrophils (G) were determined by ELISA and flow cytometry, respectively. (H) BLM-exposed mice were treated with IL-17RA-Fc or isotype control for the times indicated. Quantitative analysis of the fibrotic area by H&E and Masson's trichrome staining was performed 21 d after instillation of BLM. Data represent means ± SD of three independent determinations with BALF or lung tissues from $n = 5$ (H) or $n = 3$ mice/group for each time point (A–G).

referred to as IL-17 instead of IL-17A) at days 7, 10, and 13 after BLM treatment than did TG2$^{-/-}$ mice (Fig. 2, A and C). Thirty to forty percent of IL-17^{+} cells also expressed IL-17F, whereas all IL-17F^{+} cells coexpressed IL-17 (Fig. S2). Numbers of CD4^{+} IFN-γ^{+} T cells in WT mice were approximately twofold higher than in TG2$^{-/-}$ mice (Fig. 2, B and C). Moreover, IL-17 levels in BALF correlated with CD4^{+} IL-17^{+} T cell numbers and peaked 13 d after BLM treatment (Fig. 2 D).

To evaluate the essential role of IL-17 in inflammatory cell recruitment after exposure to BLM, we treated mice between days 0 and 10 with IL-17RA-Fc, which can block both IL-17 and IL-17F (Kuestner et al., 2007). IL-17RA-Fc treatment decreased BALF levels of IL-17 (Fig. 2 D) and numbers of CD4^{+} IL-17^{+} T cells (Fig. 2 E), as well as numbers of total inflammatory cells (Fig. 2 F) and neutrophils (Fig. 2 G). We next evaluated the effect of IL-17RA-Fc on the development of fibrosis. BLM-exposed mice treated with IL-17RA-Fc between days 0 and 10 exhibited reduced fibrosis compared with isotype control-treated animals (days 0 to 21) and a similar or greater reduction than animals treated with IL-17RA-Fc between days 0 and 21 (Fig. 2 H). This suggests that the production of IL-17 and/or IL-17F after exposure to BLM is important in the pathogenesis of lung injury, predominantly during the initial inflammatory phase. This hypothesis was confirmed by the finding that mice treated with IL-17RA-Fc between days 11 and 21 displayed similar or higher levels of fibrosis to/than those treated with isotype control between days 0 and 21 (Fig. 2 H). Thus, IL-17RA-Fc was more effective at blocking fibrosis during the first half of the treatment period.

The critical role of IL-6 during BLM-induced Th17-mediated pulmonary inflammation and fibrosis was confirmed by blocking with anti-IL-6 antibodies. Treatment between days 0 and 10 decreased the numbers of both total inflammatory cells and CD4^{+} T cells by half compared with isotype controls (Fig. 3, A and B). The reduction in CD4^{+} IL-17^{+} T cell numbers by anti-IL-6 antibody treatment was more marked: less than 15% of those in isotype control-treated mice (Fig. 3 C). This reduced inflammation was reflected in the decreased pulmonary fibrosis of these mice at 21 d after BLM instillation compared with isotype controls (Fig. 3, D and E).

Pulmonary epithelial cells are responsible for TG2-mediated IL-6 secretion after BLM treatment

TG2 is a ubiquitous enzyme expressed in both parenchymal cells and inflammatory cells. Innate immune cells, such as macrophages, are known to secrete inflammatory cytokines (including IL-6) that initiate acute inflammation after tissue injury. Moreover, TG2 activity in inflammatory cells, but not endothelial cells, was crucial to the pathogenesis of atherosclerosis induced by a high-fat diet in LDL receptor-deficient mice (Boisvert et al., 2006). However, in our study, BALF IL-6 levels peaked 3 d after BLM treatment (Fig. 1 D) and did not correlate with numbers of infiltrating inflammatory cells (Fig. 1, G, H, and J), suggesting that innate immune cells may not be the primary source of IL-6 in our model. We hypothesized that lung epithelial cells or fibroblasts may instead produce IL-6 in a TG2-dependent manner, in response to BLM-induced tissue injury. To test this, we evaluated IL-6 expression in the lungs of WT B6 mice 2–3 d after BLM treatment. Basal IL-6 expression levels in the lung were low and increased by BLM treatment. Dense immunoreactive foci were localized in the pulmonary epithelial cells, particularly in the round-shaped type II epithelial cells that expressed prosurfactant protein-C (pro-SP-C; Fig. 4 A). TG2-dependent IL-6 production from pulmonary epithelial cells was evaluated using purified epithelial cells. Sort-purified primary mouse lung epithelial cells (MLECs; purity > 90%; Fig. 4 B, left) from WT and TG2$^{-/-}$ mice were treated with BLM. Treatment with BLM for 48 h increased secretion of IL-6 by BLM-treated primary MLECs from WT, but not TG2$^{-/-}$, mice (Fig. 4 B, right). IL-6 levels in the culture supernatants of BLM-treated primary mouse lung fibroblasts (MLFs) were not greater than in PBS-treated controls of either mouse strain (Fig. 4 B, right). This selective responsiveness of epithelial cells was corroborated by the fact that BLM stimulated TG2 activity in primary MLECs, but not primary MLFs, as evaluated by Western blotting, ELISA, and fluorescence microscopy in conjunction with biotinylated pentylamine incorporation (Fig. S3, A–C). TG2-mediated IL-6 production from MLECs was confirmed by the addition of the TG2 inhibitor cysteamine (CyM). IL-6 production from WT MLECs was inhibited by CyM in a dose-dependent manner (Fig. 4 C).

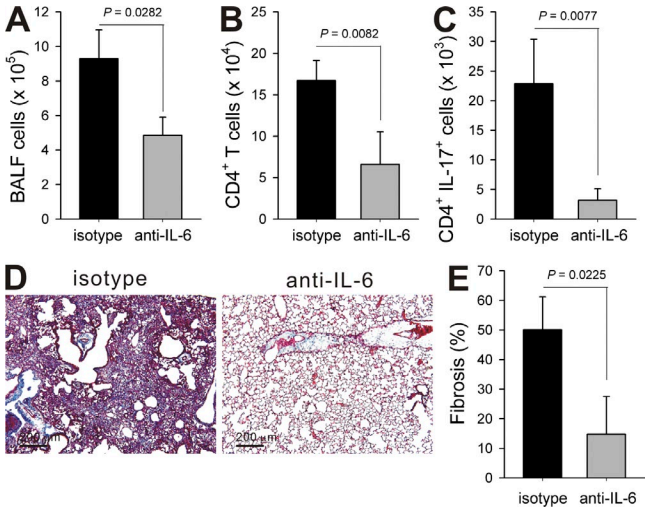

Figure 3. IL-6 blocking reduces pulmonary inflammation, Th17 responses, and fibrosis induced by BLM. (A–C) Inflammatory cells in BALF were harvested 8 d after BLM exposure. BLM-exposed WT B6 mice were treated with blocking anti–IL-6 mAb or isotype-control twice weekly, beginning 1 d before BLM treatment (100 μg/mouse, i.p.). Numbers of total cells (A), CD4^{+} T cells (B), and CD4^{+} T cells producing IL-17 (C) in BALF were determined by flow cytometry. (D) A representative photograph of lungs from isotype control– and anti–IL-6 mAb–treated WT B6 mice 21 d after BLM exposure. Sections were stained with Masson's trichrome. (E) Quantitative analysis of the fibrotic area by H&E and Masson's trichrome staining was performed 21 d after instillation of BLM. Data represent means ± SD of two independent determinations with BALF or lung tissues from n = 5 mice/group.

Published July 11, 2011

Next, the role of NF-κB activation in TG2-induced IL-6 secretion by pulmonary epithelial cells was evaluated. BLM treatment increased NF-κB reporter activity in primary MLECs from WT, but not TG2$^{-/-}$, mice (Fig. S4 A). NF-κB activity was not altered in primary MLFs from either mouse strain (Fig. S4 B). Levels of phospho-p65 in the lungs of WT mice increased 3 d after exposure to BLM and were higher than those in TG2$^{-/-}$ mice at the same time point (Fig. S4 C). Moreover, the secretion of IL-6 by primary MLECs from WT mice was suppressed by treatment with the NF-κB inhibitor Bay-11-7082 (Fig. 4 D). These data suggest that BLM induced secretion of IL-6 by lung epithelial cells through activation of a TG2-dependent NF-κB signaling pathway.

Defective Th17 responses in TG2$^{-/-}$ mice is not T cell intrinsic

Because TG2 is also expressed in T cells, the failure to trigger a Th17 response in TG2$^{-/-}$ mice may reflect a defect in the differentiation of TG2$^{-/-}$ T cells. To assess this, we induced the Th17 differentiation of lymphocytes isolated from WT and TG2$^{-/-}$ mice by addition of IL-6 and TGF-β to the

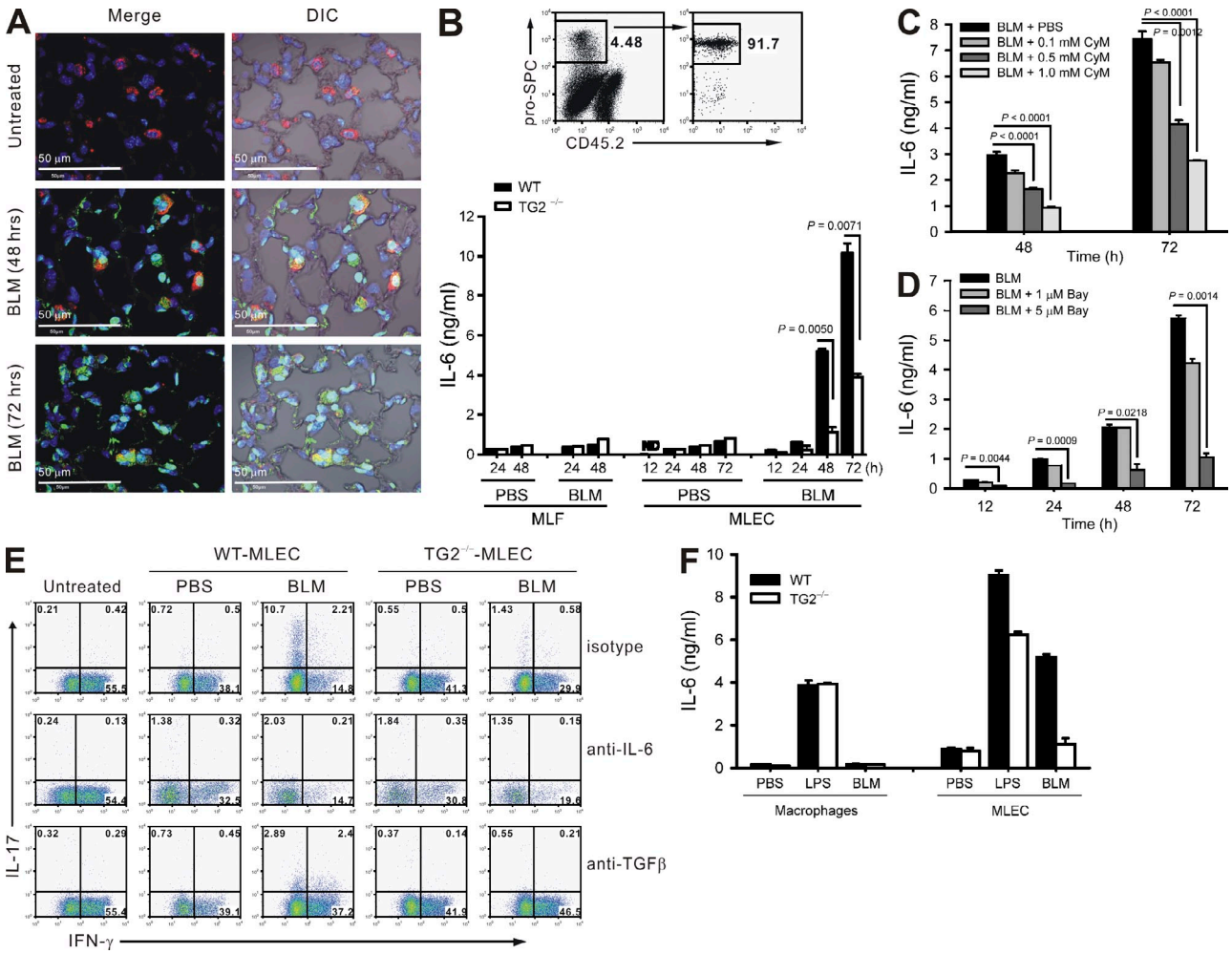

Figure 4. BLM induces secretion of IL-6 from lung epithelium. (A) Immunofluorescence staining of IL-6 production (green) from pro-SP-C (red)–expressing type II epithelial cells in the lungs of BLM-exposed WT B6 mice. Nuclei were counterstained with DAPI (blue). (B) Lung epithelial cells expressing pro-SP-C were sort-purified (top). IL-6 levels in culture supernatants of sort-purified primary MLECs and primary MLFs from WT B6 mice as determined by ELISA. Cells (2×10^4) were treated with BLM (5 µg/ml) for the times indicated. (C) Primary MLECs from WT B6 mice were treated with BLM (5 µg/ml) in the presence of the TG2 inhibitor CyM or PBS. (D) Effect of Bay-11-7082, a chemical inhibitor for NF-κB, on BLM-induced IL-6 secretion in primary MLECs from WT B6 mice. (E) Th17 differentiation of CD4$^+$ T cells induced by culture supernatants of primary MLECs. Lymphocytes isolated from WT B6 mice were stimulated with anti-CD3 and anti-CD28 for 3 d in the presence of culture supernatants of primary MLECs from WT and TG2$^{-/-}$ mice treated with PBS or BLM. As indicated, anti–IL-6 (10 µg/ml) or anti–TGF-β (10 µg/ml) antibodies were added to the culture. After restimulation with PMA and ionomycin, percentages of CD4$^+$ T cells expressing IL-17 or IFN-γ were determined by flow cytometry. (F) IL-6 levels in the culture supernatants of lung macrophages and primary MLECs were determined by ELISA. Lung macrophages (5×10^4) and primary MLECs (2×10^4) from WT B6 and TG2$^{-/-}$ mice treated with PBS, LPS (1 µg/ml), or BLM (5 µg/ml) for 48 h. (B–F) Data represent means ± SD, based on three independent determinations using samples from $n = 3$ cell cultures. *, $P \leq 0.05$; **, $P \leq 0.005$. Representative data from three independent determinations are shown.

Published July 11, 2011

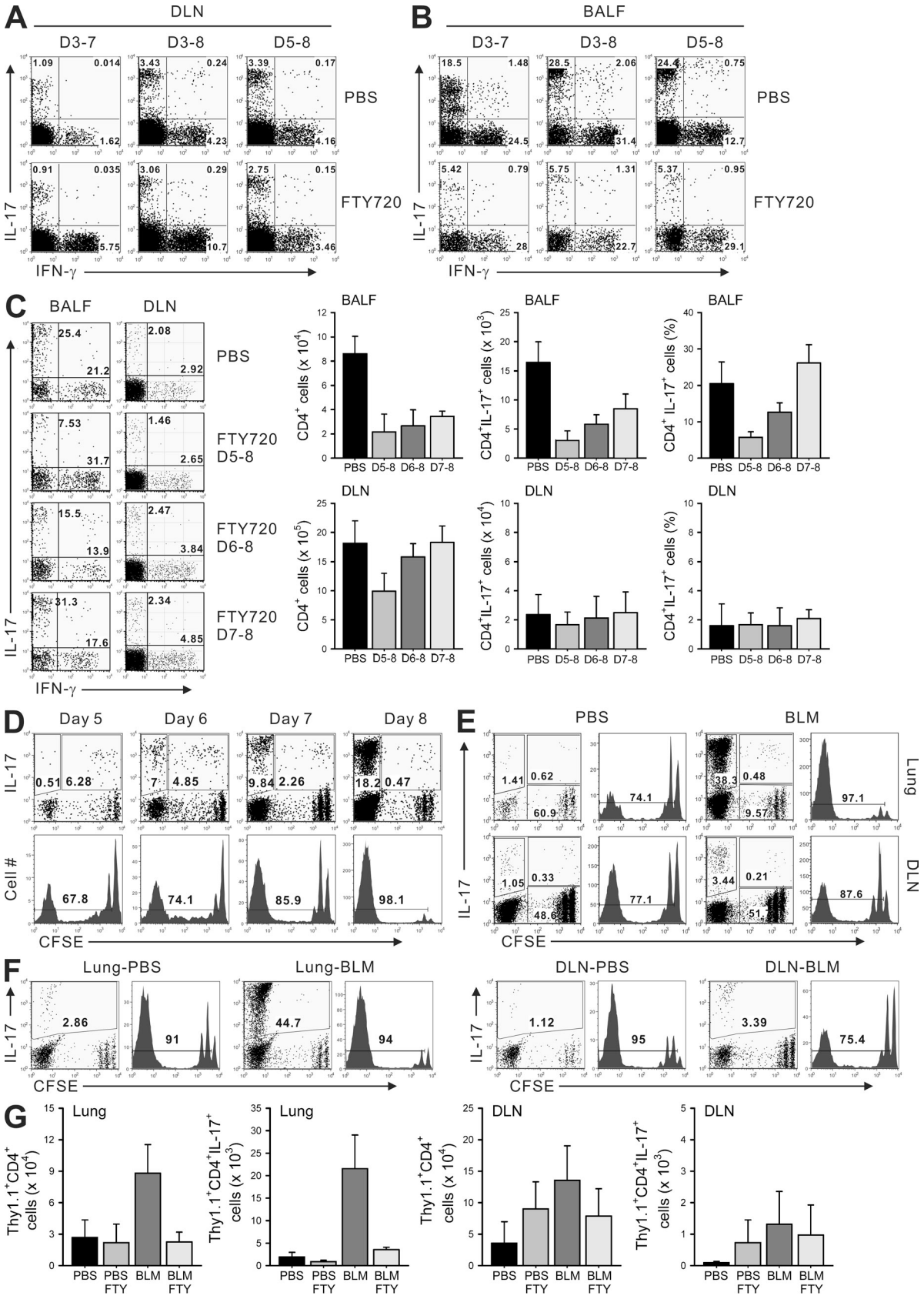

Published July 11, 2011

growth medium. We detected no difference between the percentages of $CD4^+$ T cells expressing IL-17 in WT and $TG2^{-/-}$ mice (Fig. S5 A). Moreover, TGF-β–treated T cells from $TG2^{-/-}$ mice displayed similar in vitro differentiation into regulatory T cells as did T cells from WT mice (Fig. S5 B). These findings show that defects in Th17 differentiation in $TG2^{-/-}$ mice are not T cell intrinsic. The importance of T cell-extrinsic factors for Th17 differentiation after BLM-induced injury was confirmed by applying culture supernatant from BLM-stimulated primary MLECs from WT and $TG2^{-/-}$ mice to activated $CD4^+$ T cells from WT mice. Incubation with culture supernatants from WT MLECs, but not from $TG2^{-/-}$ MLECs, increased the Th17 differentiation of $CD4^+$ T cells. These effects were abrogated by the addition of anti–IL-6 or anti–TGF-β antibodies to the culture medium (Fig. 4 E).

The TG2-dependency of IL-6 production in pulmonary epithelial cells and subsequent Th17 differentiation were the characteristic features of BLM-induced lung injury. In contrast, exposure to LPS, an infection-associated stimulus, induced secretion of IL-6 by primary MLECs and macrophages from both WT and $TG2^{-/-}$ mice (Fig. 4 F), and culture supernatants from LPS-stimulated primary MLECs both from WT and $TG2^{-/-}$ mice induced Th17 differentiation of $CD4^+$ T cells (unpublished data). Activation of epithelial TGF-β, which contributes to Th17 differentiation, after treatment with either BLM or LPS, was also independent of TG2 expression (Fig. S6 and data not shown). These results indicate that epithelial TG2 activity is crucial for IL-6 secretion and Th17 responses in noninfectious BLM-induced injury.

BLM treatment induced Th17 differentiation in the lung

In this study, we hypothesize that TG2 expressed by pulmonary epithelial cells responded to BLM treatment and induced Th17 differentiation, leading to inflammatory cascade and fibrosis. We questioned how the tissue microenvironment produced by activated pulmonary epithelial cells could lead to Th17 differentiation. One possibility is that the local microenvironment in the lung has been translated into tissue dendritic cells. Educated dendritic cells migrate into the draining lymph nodes and activate and differentiate naive T cells; differentiated Th17 cells then migrate to the inflamed lung. Another possibility is that the tissue microenvironment in the lung directly induces T cell activation and differentiation. To evaluate these possibilities, we intratracheally administered BLM, followed by application of FTY720. FTY720, a superagonist of sphingosine-1-phosphate receptor 1, inhibits the egress of T cells from, but not migration of tissue dendritic cells from inflamed tissue to, lymph nodes (Worbs et al., 2006). If BLM-induced T cell activation and differentiation occurs in the draining lymph nodes, then differentiated Th17 cells would be expected to accumulate there and would not migrate into the lung in the presence of FTY720. FTY720 treatment between days 3 and 7 (analyzed on day 7), between days 3 and 8 (analyzed on day 8), and between days 5 and 8 (analyzed on day 8) did not show accumulation of differentiated Th17 cells in the draining lymph nodes compared with PBS-treated controls (Fig. 5 A). FTY720 treatment also inhibited pulmonary Th17 differentiation, suggesting a lack of migration of unactivated T cells into the lung after FTY720 treatment (Fig. 5 B). Time-scheduled treatment of FTY720 suggested that T cell migration and Th17 differentiation in the lung occur primarily between days 5 and 8 after BLM instillation. A reduction in the numbers and percentage of $CD4^+IL\text{-}17^+$ T cells in the lung according to the serial shortening of the treatment duration of FTY720 did not lead to proportionate accumulation of these cells in the draining lymph nodes (Fig. 5 C).

We next evaluated T cell proliferation and Th17 differentiation in the lung and draining lymph nodes during this period. CFSE-labeled $Thy1.1^+CD4^+$ T cells were adoptively transferred into B6 (Thy1.2) mice 1 d after BLM instillation. Recipient mice received 300 μg of depleting anti-Thy1.2 antibody on days −1 and 2. Donor $CD4^+$ T cells in the lung showed proliferation and Th17 differentiation from day 5 after BLM instillation. A sequential increase in the percentages and numbers of donor $Thy1.1^+CD4^+$ T cells and $CD4^+IL\text{-}17^+$ cells in the lung was evident from days 5–8 after BLM instillation (Fig. 5 D). In contrast, $CD4^+$ T cell proliferation in the draining lymph nodes and spleens of BLM-administered mice was comparable to that in PBS-treated control animals, reflecting homeostatic proliferation of these cells in the lymphoid organs of T cell–depleted hosts (Fig. 5 E and not depicted). Notably, homeostatic proliferation did not

Figure 5. Th17 cells proliferate and differentiate in the lung. (A and B) WT B6 mice received BLM intratracheally (1.5 mg/kg). BLM-exposed mice were treated with PBS or FTY720 (2 mg/kg/day, i.p.) between days 3 and 7 (analyzed on day 7), between days 3 and 8 (analyzed on day 8), and between days 5 and 8 (analyzed on day 8). Mice were sacrificed and BALF and draining lymph nodes (DLN) harvested on the days noted above. The percentages of $CD4^+$ cells producing IL-17 or IFN-γ in draining lymph nodes (DLN; A) and BALF (B) were determined by flow cytometric analysis. (C) BLM-exposed WT B6 mice were treated with PBS or FTY720 (2 mg/kg/day, i.p.) at day 5, 6, or 7 after BLM-exposure. Numbers and percentages of $CD4^+$ cells producing IL-17 in BALF and DLN were determined by flow cytometric analysis 8 d after BLM exposure. (D and E) WT B6 (Thy1.2) mice received BLM intratracheally (1.5 mg/kg). On the next day, BLM-exposed mice were adoptively transferred with CFSE-labeled $Thy1.1^+$ $CD4^+$ T cells (5×10^6 cells). To deplete endogenous T cells, anti-Thy1.2 antibody (30-H12; 300 μg/mouse) was administered i.p. to recipient mice on days −1 and 2 of BLM treatment. (D) Mice were sacrificed to harvest leukocytes from lungs on the days indicated. The percentages of donor $Thy1.1^+$ $CD4^+$ cells producing IL-17 were determined by flow cytometric analysis. (E) The percentages of donor $Thy1.1^+$ $CD4^+$ cells producing IL-17 in lungs and draining lymph nodes (DLN) of recipient mice were determined by flow cytometric analysis 8 d after PBS or BLM exposure. (F and G) WT B6 (Thy1.2) mice were adoptively transferred with CFSE-labeled naive phenotype $Thy1.1^+$ $CD4^+$ T cells (5×10^6 cells) 1 d after BLM exposure. Some mice received FTY720 10 h before naive phenotype $Thy1.1^+$ $CD4^+$ T cell transfer. Percentages (F) and numbers (G) of donor $Thy1.1^+$ $CD4^+$ cells producing IL-17 in lungs and DLN of recipient mice were determined by flow cytometric analysis 8 d after PBS or BLM exposure. (C and G) Data represent means ± SD of three independent determinations with BALF or lung tissues from $n = 5$ mice/group.

induce Th17 differentiation in either the lung or the draining lymph nodes (Fig. 5 E). Transfer of sort-purified Thy1.1$^+$ CD4$^+$CD45RB^{hi} (naive phenotype) cells also revealed comparable donor CD4$^+$ T cell proliferation and Th17 differentiation in the lung (Fig. 5 F). The effect of FTY720 on naive phenotype CD4$^+$ T cell recruitment into the lung was evaluated by treating with FTY720 during the whole experimental period. Increased numbers of donor CD4$^+$ and CD4$^+$IL-17$^+$ T cells after BLM treatment were blocked by FTY720 treatment (Fig. 5 G), indicating that migration of unactivated T cells into the lung was blocked by FTY720 treatment. In the draining lymph nodes, FTY720 treatment, again, did not lead to the accumulation of donor CD4$^+$ and CD4$^+$IL-17$^+$ T cells after naive phenotype CD4$^+$ T cell transfer and BLM treatment (Fig. 5 G).

Epithelial TG2 is critical for Th17 responses and fibrosis

To further confirm the role of the lung epithelium and epithelial TG2 in Th17 responses in vivo, BM-chimeric mice were exposed to BLM, and numbers of cells in BALF were analyzed 10 d later. WT mice reconstituted with TG2$^{-/-}$ BM (BM$^{TG2-/-}$→WT) exhibited a similar percentage of CD4$^+$ IL-17$^+$ cells to WT control chimeras (BM^{WT}→WT), whereas TG2$^{-/-}$ mice reconstituted with WT BM (BM^{WT}→TG2$^{-/-}$) displayed reduced percentages of CD4$^+$ IL-17$^+$ cells that were comparable to those in TG2$^{-/-}$ control chimeras (BM$^{TG2-/-}$→TG2$^{-/-}$; Fig. 6 A). Th17 differentiation in the chimeras correlated with BALF IL-6 levels (Fig. 6 B). Histopathological analysis 21 d after BLM treatment revealed fewer inflammatory cells and reduced collagen deposition in the lungs of chimeras in which TG2$^{-/-}$ mice were the recipients (BM^{WT}→TG2$^{-/-}$ and BM$^{TG2-/-}$→TG2$^{-/-}$), compared with those in which WT mice were the recipients (BM^{WT}→WT and BM$^{TG2-/-}$→WT; Fig. 6 C). Similarly, fibrosis, expressed as percentage of fibrotic tissue (as assessed by Masson's trichrome staining; Fig. 6 D), and collagen content (Fig. 6 E) were reduced in the TG2$^{-/-}$ host chimeras (BM^{WT}→TG2$^{-/-}$ and BM$^{TG2-/-}$→TG2$^{-/-}$). Collectively, these results indicate that nonhematopoietic (i.e., epithelial) TG2 is important for generation of the local Th17 response and subsequent fibrosis that follows BLM-induced tissue injury.

Fibroblast-derived TG2 mediates TGF-β–induced fibrogenesis

Chronic inflammation induces TGF-β activation, which, in turn, dampens the inflammatory response (Serhan and Savill, 2005; Li et al., 2006). We found the bioactivity of TGF-β in the BALF of BLM-exposed WT mice to be significantly higher than that in similarly treated TG2$^{-/-}$ mice (Fig. S7 A). This increase displayed similar kinetics to that of inflammatory cell infiltration (Fig. 1, G–J), peaking at day 10 after BLM exposure (Fig. S7 A). Consistent with these findings, the bioactivity of TGF-β in the BALF of WT mice reconstituted with TG2$^{-/-}$ BM (BM$^{TG2-/-}$→WT) was markedly higher than that in TG2$^{-/-}$ mice reconstituted with WT BM (BM^{WT}→TG2$^{-/-}$; Fig. S7 B), a response that mirrors inflammatory cell recruitment in these chimeras (Fig. 6, A and B). Thus, epithelial TG2 induced an inflammatory cascade, comprising Th17 induction and TGF-β activation.

We next evaluated the role of fibroblast-derived TG2 in the effector phase of fibrogenesis. TGF-β treatment increased the expression and cross-linking of the ECM protein fibronectin in primary MLFs from WT mice, but not from TG2$^{-/-}$ animals (Fig. S8, A and B). Furthermore, TGF-β–mediated increases in TG2 activity, fibronectin expression, and cross-linking, as well as α-SMA expression in IMR90 human

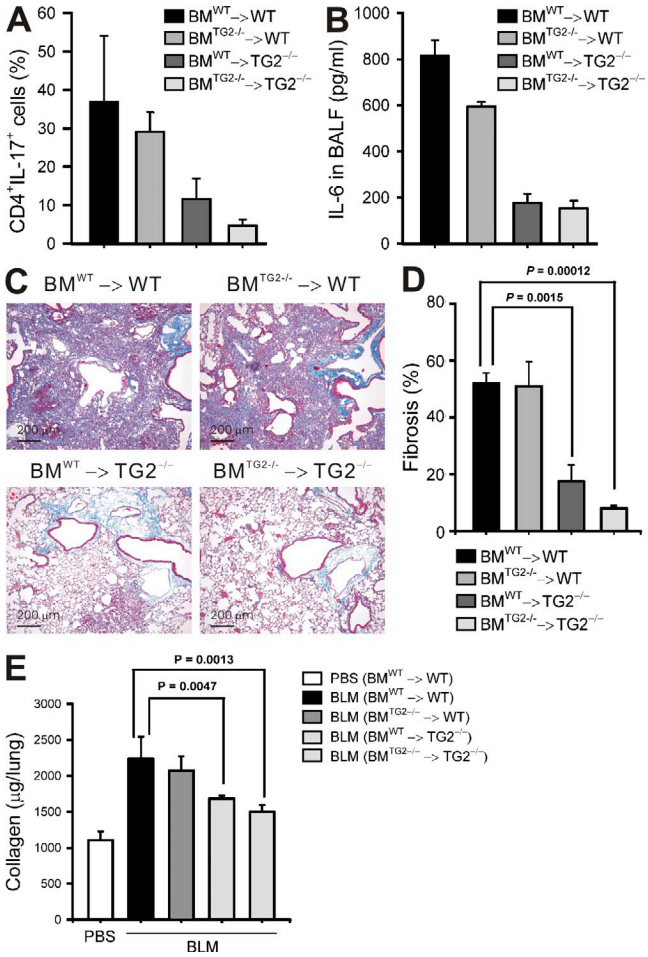

Figure 6. Chimeric mice with TG2$^{-/-}$ recipients exhibit diminished pulmonary inflammation and fibrosis in response to BLM. BM chimeras were prepared by irradiation of WT B6 or TG2$^{-/-}$ mice, followed by T cell–depleted BM cell reconstitution (BM^{WT}→WT, BM$^{TG2-/-}$→WT, BM^{WT}→TG2$^{-/-}$, and BM$^{TG2-/-}$→TG2$^{-/-}$). (A) The percentage of CD4$^+$ IL-17$^+$ cells in BALF of the chimeras was determined by flow cytometric analysis 10 d after BLM exposure. (B) IL-6 levels in BALF from chimeras 3 d after BLM exposure was determined by ELISA. (C) Representative photographs of lungs from chimeras are shown. Lung tissues were prepared 21 d after BLM instillation and stained with Masson's trichrome. (D and E) Quantitative analysis of fibrosis was performed using Masson's trichrome staining (D) and pulmonary collagen content (Sircol assay; E) 21 d after BLM exposure. Data represent means ± SD of three independent determinations with BALF or lung tissues from n = 5 mice/group.

Published July 11, 2011

fibroblasts, were inhibited by the TG2 inhibitor CyM (Fig. S9, A and B). These results indicate that TG2 is a downstream effector of TGF-a responses in fibroblasts during wound healing/fibrosis.

Inhibition of TG2 during either the early or late phases ameliorates lung fibrosis

We have shown that TG2 is very important in both the initial inflammatory phase and subsequent fibrosis phase in our BLM-induced lung fibrosis model. Because clinical cases of pulmonary fibrosis are characterized by both inflammation and wound healing/fibrosis, and the inhibition of either process alone using antiinflammatory or antifibrotic drugs does not adequately reduce disease progression (Rogliani et al., 2008; Kim and Meyer, 2008; du Bois, 2010), the distinct roles of TG2 in both processes are intriguing and warrant further evaluation. We assessed the effects of inhibiting TG2 during the *early and late* phases on the development of lung fibrosis. BLM-exposed mice treated with CyM between days 0 and 10 exhibited markedly reduced leukocyte infiltration and fibrosis, comparable to mice treated with CyM between days 0 and 21, as evaluated by histopathological analyses (Fig. 7 A), measurements of fibrotic areas (Fig. 7 B), and total lung collagen content (Fig. 7 C). Mice treated with CyM between days 11 and 21 also exhibited significantly reduced fibrosis relative to animals treated with vehicle between days 0 and 21 (Fig. 7, A–C). We also observed significantly reduced fibrosis in mice treated with CyM between days 15 and 28 compared with animals treated with vehicle alone between days 15 and 28 in a 28-d BLM-induced lung fibrosis model (Fig. S10).

DISCUSSION

A causal role for TG2 in pathological increases in collagen deposition in the kidney and liver has been proposed; specifically, TG2 is considered to be important in the development of fibrosis in these organs (Shweke et al., 2008; Elli et al., 2009). Originally described as an enzyme that irreversibly cross-links ECM proteins, TG2 has recently been shown to play an active role in inflammation (Kim, 2006). Here, we used a BLM-induced pulmonary fibrosis model to demonstrate that activation of epithelial TG2 induces a Th17 inflammatory response in the lung that causes excessive wound healing and fibrosis through activation of fibroblast TG2. We have shown that TG2 is a critical regulator of inflammatory and repair responses and links noninfectious tissue injury and fibrogenesis.

In this study, we identified a critical role for epithelial cell–derived TG2 in inducing the secretion of IL-6, and consequent Th17 inflammation, after BLM-induced lung damage. During protective immunity against pathogens and autoimmune tissue destruction, IL-6 secreted by innate immune cells is thought to activate Th17 differentiation (Weaver et al., 2007; McGeachy and Cua, 2008; Korn et al., 2009). However, we found that WT lung epithelial cells treated with BLM produced IL-6, and that soluble factors secreted from BLM-exposed lung epithelial cells induced Th17 differentiation. These effects were blocked by anti–IL-6 and anti–TGF-β antibodies, indicating that IL-6 and TGF-β are the primary cytokines involved in Th17 differentiation after BLM-induced lung injury. Treatment with a blocking anti–IL-6 antibody in vivo also confirmed the critical role of IL-6 in Th17-mediated pulmonary inflammation and fibrosis.

In contrast, culture supernatants from BLM-stimulated lung epithelial cells from $TG2^{-/-}$ mice contained only low levels of IL-6 and did not support Th17 differentiation. The critical involvement of epithelial TG2 in Th17 responses in vivo was further confirmed in our BM chimera study. As anticipated, WT recipients produced greater amounts of IL-6 than $TG2^{-/-}$ recipients. In WT mice reconstituted with WT or $TG2^{-/-}$ BM cells, 30–50% of $CD4^+$ T cells produced IL-17, whereas very few $CD4^+$ $IL\text{-}17^+$ cells were present in $TG2^{-/-}$ recipients. Although this disparity may stem from differences in the amount of IL-6 secreted by epithelial cells, IL-6 production is not always TG2-dependent. In an LPS-induced septic shock model, both WT and $TG2^{-/-}$ mice rapidly secreted large amounts of IL-6 and IFN-γ (Falasca et al., 2008). In the present study, LPS

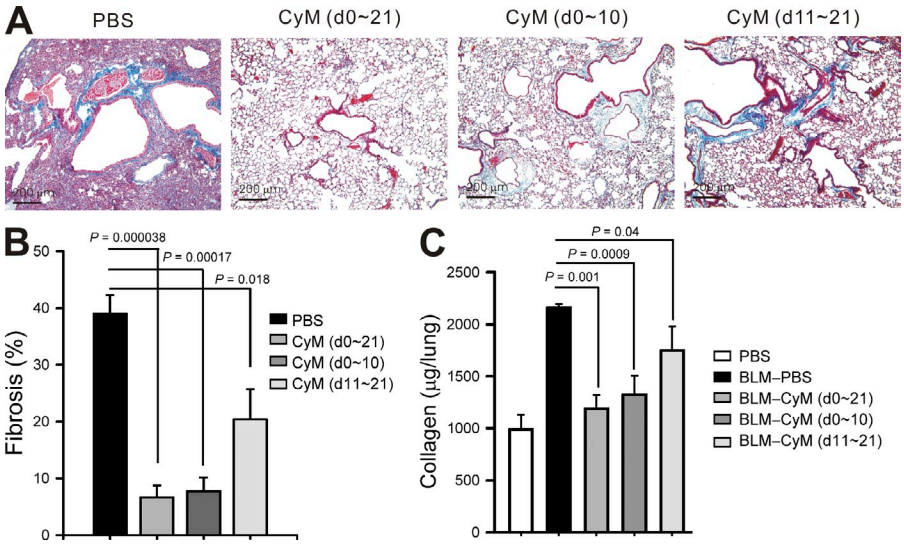

Figure 7. Inhibition of TG2 by CyM during either the early or late phase effectively reduces lung fibrosis induced by BLM. (A) Representative photographs of lungs from WT mice 21 d after exposure to BLM. BLM-exposed mice were treated with PBS or CyM (40 mg/kg/day, i.p.) during the early phase (days 0–10), late phase (days 11–21), or for all 21 d. Sections were stained with Masson's trichrome. (B and C) Quantitative analysis of fibrotic area (B) and pulmonary collagen content (C) 21 d after BLM exposure. Data represent means ± SD of three independent determinations with lung tissues from n = 5 mice/group for each time point.

induced the secretion of IL-6 from both lung epithelial cells and lung macrophages in a TG2-independent manner. Bacterial molecules activated epithelial and inflammatory cells directly through TLRs in a process that seemed to be TG2 independent.

In conclusion, TG2-dependent epithelial IL-6 production is a defining characteristic of noninfectious epithelial injury. TG2 serves as a stress sensor in epithelial cells (Ientile et al., 2007) and transduces epithelial damage into IL-6 secretion, which provides the signal for inflammatory Th17 differentiation after noninfectious injury. Epithelium-derived IL-6 may also modulate the local balance between Th17 and regulatory T cells, and thus influence immune homeostasis (Ivanov et al., 2007). The role of TG2 in this context requires further investigation, especially under noninfectious conditions. Th17 cells have been implicated in various autoimmune diseases, including multiple sclerosis (Kebir et al., 2007) and psoriasis (Di Cesare et al., 2009), and it will be interesting to determine whether the activation of TG2 promotes Th17 differentiation in such diseases.

T cell activation and Th17 differentiation in the lung after BLM instillation requires further comment. In this study, we obtained an unexpected finding that $CD4^+$ T cell proliferation and Th17 differentiation occurred primarily in the lung, not in the draining lymph nodes, after BLM-mediated pulmonary epithelial injury. A long-standing immunological paradigm is the central sensitization of naive T cells in the lymphoid organs, which reflects the characteristic migratory pathway of naive T cells confined to these sites (Dailey, 1998). For this reason, $CD4^+$ T cell activation and differentiation in the peripheral tissue is intriguing, and recent studies showing that naive T cells also migrate to peripheral tissues, including the lung (Cose et al., 2006; Staton et al., 2006), further confirm our data; adoptive transfer of naive phenotype $CD4^+$ donor T cells revealed $CD4^+$ T cell proliferation and Th17 differentiation in the lung after BLM instillation, and FTY720 treatment did not lead to accumulation of donor $CD4^+$ and $CD4^+$IL-17^+ T cells in the draining lymph nodes. Immune activation and amplification in peripheral tissues is considered to be significant for perpetuating chronic inflammation; i.e., ectopic lymphoid structures in the joints in rheumatoid arthritis (Manzo and Pitzalis, 2007). Moreover, migration to and activation of naive tumor-specific $CD8^+$ T cells inside the tumor tissue has warranted proposal of a new pathway, where naive T cells can be activated by interaction with tissue-resident cells (Thompson et al., 2010). In this study, naive $CD8^+$ T cells were activated both by tumor cells themselves and by cross-presenting antigen-presenting cells within the tumor (Thompson et al., 2010). The nature of the tissue-resident cells in the lungs of BLM-administered mice that provide such signals has not been determined. As is the case in tumor tissue, pulmonary epithelial cells themselves or cross-presenting tissue-resident antigen-presenting cells may perform this function. Naive $CD4^+$ T cell migration, activation, and differentiation in the inflamed lung may thus serve as a novel pathway of peripheral activation of naive T cells after epithelial tissue injury. The characteristic tissue microenvironment of the lung, or induced lymphoid-like structures in this tissue, may be responsible for this. The importance of other mucosal tissues for activation of naive T cells warrants further investigation. Such alternate T cell activation pathways may provide new methods for regulation of immune responses.

Th17 lymphocytes mediate lung inflammation by regulating neutrophil recruitment (Aujla et al., 2007; Weaver et al., 2007; McGeachy and Cua, 2008; Korn et al., 2009). Here, we demonstrated that induction of a Th17 response is critical during the initial inflammatory cascade that follows intratracheal BLM instillation, consistent with recent works (Sonnenberg et al., 2010; Wilson et al., 2010). Recruitment of inflammatory cells, most notably neutrophils, paralleled this Th17 response, whereas blocking IL-17 signaling through the administration of IL-17RA-Fc between days 0 and 10 greatly reduced inflammatory cell/neutrophil recruitment. IL-17RA-Fc treatment also reduced lung fibrosis measured at day 21, consistent with previous studies that neutrophil activation and elastase production are critical to the pathogenesis of BLM-induced lung fibrosis (Jones et al., 1998; Chua et al., 2007). However, treatment with IL-17RA-Fc during the late phase (days 11 to 21) increased fibrosis by 1.4-fold compared with isotype control-treated mice. Initial amplification of the inflammatory response and subsequent negative regulatory effects of IL-17 were previously reported in allergic asthma (Schnyder-Candrian et al., 2006). IL-17 secreted by $\gamma\delta$ T cells has been shown to provide a help signal during pulmonary epithelial repair (Braun et al., 2008). This pathway may contribute to the responses we observed in this study. Indeed, an essential role for IL-17A in lung inflammation, but not fibrosis, has also been reported in another noninfectious injury model of experimental silicosis (Lo Re et al., 2010).

In addition to the dominant role of IL-17, other cytokines such as IFN-γ, IL-1β, IL-13, TGF-β, IL-10, and IL-4 have also been implicated in the BLM-induced pulmonary fibrosis model (Wilson et al., 2010). IFN-γ was reported to have a critical role during BLM-induced pulmonary fibrosis (Chen et al., 2001), and we also found that numbers of $CD4^+$ IFN-γ^+ T cells in WT mice were approximately twofold higher than in $TG2^{-/-}$ mice. However, there was a dramatic reduction in $CD4^+$ IL-17^+ T cells compared with $CD4^+$ IFN-γ^+ T cells in $TG2^{-/-}$ mice. Nonetheless, our data showed that the reduction of pulmonary fibrosis in IFN-$\gamma^{-/-}$ mice was not dramatic compared with $TG2^{-/-}$ mice (unpublished data), and blocking the IL-17 signaling pathway through IL-17RA-Fc treatment almost completely abrogated lung inflammation, leading us to consider that IL-17 rather than IFN-γ plays a predominant role during the initial inflammation after BLM instillation. A recent work showing the predominant role of IL-17A in the BLM-induced lung fibrosis model (Wilson et al., 2010) also supports our contention. These authors showed that IL-17A–driven fibrosis is facilitated by IFN-γ, and that the reduced fibrotic response in IFN-$\gamma^{-/-}$ mice was associated with decreased IL-17A expression and reduced circulating neutrophils (Wilson et al., 2010), which is preferable

for the dominant role of IL-17 in the BLM-induced lung fibrosis model.

In the BLM-treated lung, amplification of the initial inflammatory response as a result of Th17 polarization results in activation of TGF-β, which would be expected to dampen local inflammation and facilitate the shift to fibrogenesis (Serhan and Savill, 2005; Li et al., 2006). TGF-β acts as a fibrogenic switch that increases ECM synthesis and reduces the activity of ECM-degrading enzymes (Serhan and Savill, 2005; Li et al., 2006). It also induces expression of proteins that stabilize the ECM, including plasminogen activator inhibitor-1 and TG2 (Verderio et al., 2004). When intracellular TG2 is activated, it localizes to the marginal zone and is secreted (Gaudry et al., 1999). Extracellular TG2 acts as an ECM remodeler that increases the cross-linking of ECM molecules (Akimov and Belkin, 2001;Verderio et al., 2004). Intriguingly, intracellular TG2 activity has been suggested to be critical in renal fibrosis after subtotal nephrectomy (Johnson et al., 1997). In the present study, we found that intracellular TG2 activity in fibroblasts mediated the majority of the fibrogenic effects of TGF-β, including the synthesis of fibronectin and α-smooth muscle actin. The fibrogenic effects of TGF-β were decreased by the TG inhibitor CyM and were not observed in primary MLFs from $TG2^{-/-}$ mice. Thus, we suggest that during the fibrogenesis of lung fibroblasts, activated TGF-β exerts its effects in a primarily TG2-dependent manner.

The direct involvement of TG2 in the effector fibrogenic pathway downstream of TGF-β indicates that inhibition of TG2 may directly reduce fibrosis regardless of the presence or absence of active inflammation, a conclusion that is highly relevant to IPF, in which overt inflammation is not common (Kim and Meyer, 2008; Rogliani et al., 2008; du Bois, 2010). CyM treatment during the late phase alone in our BLM-induced lung fibrosis model significantly reduced lung fibrosis and collagen deposition. The much greater effect of CyM in mice treated during the early phase suggests that the inflammatory response is more dominant in BLM-treated mice than in human IPF patients. Thus, TG2 inhibition may modulate two essential pulmonary fibrosis pathways simultaneously and TG2 itself may represent an ideal molecular target in IPF, and inhibitors specific for TG2 may be useful tools in the treatment of pulmonary fibrotic diseases including IPF. But despite all this, the BLM-induced lung fibrosis model is an inflammation-oriented fibrosis model that may not be an ideal representation of human IPF, and inflammation and subsequent fibrosis processes may continue even in the late phase of the disease model. Therefore, it would be better to use a more fibrosis-oriented model to demonstrate the critical role of TG2 in inflammation-independent pulmonary fibrogenesis.

MATERIALS AND METHODS

Mice. B6 mice were obtained from The Jackson Laboratory. $TG2^{-/-}$ mice (De Laurenzi and Melino, 2001) were backcrossed to B6 mice for 12 generations (N12). 8–12-wk-old male mice were used for experiments, and all mice, including WT B6, were bred and maintained at the animal facility of Seoul National University College of Medicine. All animal experiments were performed with the approval of the Institutional Animal Care and Use Committee at Seoul National University.

Induction of pulmonary fibrosis. Pulmonary fibrosis was induced by intratracheal instillation with BLM (1.5 mg/kg, Nippon Kayaku, Japan) in 50 μl PBS as described previously (Jones et al., 1998). A proportion of the mice were injected intraperitoneally with CyM (40 mg/kg/day; Sigma-Aldrich), recombinant murine IL-17RA-Fc (100 μg/mouse/day; R&D Systems) or control human IgG1 (100 μg/mouse/day; R&D Systems) suspended in PBS. To block IL-6 signaling, mice were injected intraperitoneally with blocking anti–IL-6 mAb (100 μg/mouse; eBioscience) or control Rat IgG1 (100 μg/mouse; eBioscience) every 3 d, starting 1 d before receiving BLM treatment). To evaluate Th17 differentiation in the lung, BLM-exposed mice were treated with PBS or FTY720 (2 mg/kg/day, i.p.) during the periods indicated.

BM chimera. Recipient mice were lethally irradiated (950 rad whole-body irradiation in two split doses) and injected intravenously with T cell–depleted BM cells (3×10^6/mouse), as described previously (Surh et al., 1997). Reconstituted mice were used in the experiments 10 wk after BM cell transfer.

Donor $CD4^+$ T cell analysis. WT B6 mice received an intratracheal instillation of BLM (1.5 mg/kg). 1 d later, mice were injected with 5×10^6 purified and CFSE-labeled $CD4^+$ T cells from B6.Thy1.1 lymph nodes via the tail vein. To deplete endogenous T cells, anti-Thy1.2 antibody (30-H12, 300 μg/mouse) was administered i.p. to recipient mice on days −1 and 2 of BLM treatment. For the transfer of naive phenotype $CD4^+$ T cells, cells from B6.Thy1.1 lymph nodes were labeled with APC-conjugated anti-CD4 and PE-conjugated anti-CD45RB. $CD4^+CD45RB^{high}$ cells were purified using a FACS Aria cell sorter (BD) and subsequently labeled with CFSE.

Histopathology and immunofluorescence of lung tissue. Lung tissues were fixed in 4% paraformaldehyde, processed, and embedded in paraffin. Sections were stained with H&E for histopathological analysis or with Masson's trichrome for the evaluation of collagen content and distribution. The extent of fibrosis was measured using the ProgRes CF system (Jenoptik). To investigate IL-6 expression in epithelial cells, lung tissue from BLM-exposed mice was stained with anti–IL-6 (R&D Systems) and anti–pro-surfactant protein-C (pro-SP-C; Millipore). Alexa Fluor 488–conjugated donkey anti–goat IgG (Invitrogen) and Alexa Fluor 546–conjugated anti–rabbit IgG (Invitrogen) antibodies were used for visualization. Image acquisition and processing was performing using a confocal fluorescence microscope (Olympus) and FV10-ASW 2.0 Viewer (Olympus).

Collection of BALF. Bronchoalveolar lavage was performed with five 1.0-ml aliquots of PBS through a tracheal cannula. To evaluate cytokine production, BALF cells were harvested and restimulated with 50 ng/ml PMA and 1 μg/ml ionomycin (Sigma-Aldrich) for 4 h. For intracellular staining, brefeldin A (BD) was added during the final 2 h of stimulation. Cells were fixed with 4% paraformaldehyde, permeabilized with 0.5% Triton X-100, and incubated with anti-CD4, anti-CD8, anti-IL-17, and anti–IFN-γ antibodies (eBioscience). Intracellular cytokine levels were assayed by flow cytometry.

Collagen content measurement. The total collagen content of the left lung was measured by the Sircol collagen dye binding assay, according to the manufacturer's instructions (Biocolor Ltd.).

Flow cytometry. BALF cells were incubated with mAbs to mouse CD4, CD8α, B220, CD11c, CD11b, Gr1, and F4/80 that were conjugated to fluorescein, phycoerythrin, PerCP-Cy5.5, or allophycocyanin (eBioscience). Cells were analyzed using a FACSCalibur (BD) and FlowJo software (Tree Star).

Primary lung epithelial cells. The lungs were perfused with PBS and digested with collagenase D (400 μg/ml; Invitrogen), dispase (50 μg/ml; Invitrogen), and DNase I (0.5 U/ml; Sigma-Aldrich) for 1 h at 37°C. Cells were

suspended in 30% Percoll, layered onto the top of a 70% Percoll gradient and centrifuged (800 *g*, 20 min, 4°C). The top layer, an enriched population of epithelial cells and fibroblasts, was retained. Cells were labeled with FITC-conjugated anti-Ly5.2 (eBioscience) and anti–pro-SP-C (Millipore) mAbs, followed by PE-conjugated anti–rabbit IgG. Pro-SP-C–expressing epithelial cells were subsequently purified using a FACSAria cell sorter (BD) and epithelial cell purity after sorting was >90%. Cells were maintained in Keratinocyte Basal Medium (KBM; Lonza). For isolation of fibroblast-like cells, cells were harvested after Percoll gradient centrifugation, and labeled with biotinylated anti-Ly5.2 antibody, followed by streptavidin microbeads (Miltenyi Biotech). The negative fraction was collected using an LS magnetic column. Cells were allowed to adhere to a culture dish for 1 h at 37°C and nonadherent cells were removed. Adherent fibroblast-like cells (MLFs) were maintained in DME containing 10% FBS. The second passage of these cells was used for experiments.

Transglutaminase assay. Intracellular TG2 activity was evaluated by assay of 5-(biotinamido) pentylamine (BP) incorporation into cellular proteins. Primary MLECs and MLFs were incubated with 1 mM BP for 1 h before harvesting. The cell homogenates were coated onto microtiter plates, and BP-labeled proteins were assayed by ELISA. Primary MLECs of WT B6 mice were cultured on chamber slides, treated with BLM (5 μg/ml), and incubated with 0.1 mM BP for the final hour of the culture period. TG2 activity was assessed visually using Alexa Fluor 488–conjugated streptavidin (DAKO).

In vitro differentiation of effector T cells. Lymphocytes isolated from lymph nodes were stimulated with anti-CD3 and anti-CD28 (1 μg/ml each; BD) in the presence of IL-6 (10 ng/ml; eBioscience) and TGF-β1 (5 ng/ml; R&D Systems) for 3 d, or anti-CD3 (1 μg/ml) in the presence of TGF-β1 (0.2–5.0 ng/ml) for 3 d. Cells were harvested and restimulated with PMA (50 ng/ml) and ionomycin (1 μg/ml) for 4 h. For intracellular staining, brefeldin A (1 μg/ml, Sigma-Aldrich) was added during the final 2 h of stimulation. Cells were then fixed with 4% paraformaldehyde, permeabilized with 0.5% Triton X-100, and incubated with anti-CD4, anti-CD8, anti-IL-17, anti-IFN-γ, or anti-Foxp3 mAbs (eBioscience).

ELISA. BALF or cell culture supernatants were analyzed for mouse IL-6, IL-17, MCP-1, MCP-3, and TGF-β1 (R&D systems) levels by sandwich ELISA (Lee et al., 1999).

NF-κB and TGF-β assay. Primary mouse MLECs or MLFs were co-transfected with p3κB-Luc and pRL-TK reporter constructs (Promega) for 24 h and then treated with BLM at various concentrations. Luciferase activity was assayed using a kit (Promega) with a Victor3 plate reader (Perkin Elmer) and normalized against renilla luciferase activity. To evaluate bioactivity of TGF-β, NIH-3T3 cells were co-transfected with pGL3-PAI1TRE-Luc and pRL-TK reporter constructs for 24 h, and then incubated with BALF obtained from BLM-treated mice or media supernatants for various lengths of time. Luciferase activity was assayed using a kit and normalized against renilla luciferase activity.

RNA analysis. Total RNA was isolated from lung tissues using TRIzol (Invitrogen). cDNA generated from 1 μg of total RNA by Superscript II (Invitrogen) was analyzed by Q-PCR using Assay-on-Demand TaqMan probes with primers for TG2, TGF-β1, and GAPDH (Applied Biosystems) and an ABIPRISM 7900HT Sequence Detector (Perkin Elmer). All data were normalized to the respective 18s rRNA expression. The following primer pairs were used for semiquantitative PCR: IL-6, 5′-GACAAAGCCAGAGTCCTTCAGAG-3′/5′-CTAGGTTTGCCGAGTAGATCTC-3′; MCP-1, 5′-AGGTCCCTGTCATGCTTCTG-3′/5′-TCTGGACCCATTCCTTCTTG-3′; TNF, 5′-AAGGGATGAGAAGTTCCCAA-3′/5′-AGAACCTGGGAGTAGACAA-3′; MIP-1α, 5′-ATGAAGGTCTCCACCACTGC-3′/5′-CCCAGGTCTCTTTGGAGTCA-3′; MIP-2, 5′-AGTGAACTGCGCTGTCAATG-3′/5′-TTCAGGGTCAAGGCAAACTT-3′; and IP-10, 5′-AAGTGCTGCCGTCATTTTCT-3′/5′-GTGGCAATGATCTCAACACG-3′. PCR products were analyzed by resolution on a 2% agarose gel followed by densitometric analysis (Labworks 4.6; UVP BioImaging Systems).

Western blots. Cells were harvested in a lysis solution containing 50 mM Tris/HCl (pH 7.6), 1% NP-40, 150 mM NaCl, 2 mM EDTA, and 100 μM PMSF in the presence of a protease inhibitor cocktail (Roche) and phosphatase inhibitor (Sigma-Aldrich). After incubation on ice for 30 min, cellular debris was removed by centrifugation (10 min, 4°C). Protein concentrations were assayed using the BCA protein assay reagent (Thermo Fisher Scientific). Total protein was resolved by SDS-PAGE, and then transferred to polyvinylidene difluoride membranes. After blocking with 5% skim milk, membranes were probed with the appropriate antibody. Blots were developed with an enhanced chemiluminescence Western blotting detection system (GE Healthcare). Antibodies used were as follows: anti-TG2 (Neomarker), anti-p65 (Abcam), anti–phospho-p65 (Cell Signaling technology), anti–α-smooth muscle actin (DAKO), anti-actin (Sigma-Aldrich), and anti-fibronectin (Santa Cruz Biotechnology, Inc.).

Statistical analysis. Statistical significance was analyzed using the Student's *t* test. A p-value of <0.05 was taken to indicate statistical significance.

Online supplemental material. Fig. S1 shows semiquantitative RT-PCR analysis of cytokine and chemokine expression in the lungs of BLM-exposed mice. Fig. S2 shows that 30–40% of IL-17$^+$CD4$^+$ T cells coexpress IL-17F. Fig. S3 shows TG2 expression and activity in primary MLECs and primary MLFs after BLM treatment. Fig. S4 describes NF-κB reporter activity in primary MLECs after BLM treatment. Fig. S5 shows in vitro differentiation of Th17 and regulatory T cells. Fig. S6 shows TGF-β bioactivity from primary macrophages and primary MLECs stimulated with LPS and BLM. Fig. S7 shows the bioactivity of TGF-β in the BALF of BLM-exposed mice. Fig. S8 shows the expression of fibronectin and TG2 in primary MLF after TGF-β treatment. Fig. S9 shows increased TG2 activity and α-SMA expression in human fibroblasts after TGF-β treatment. Fig. S10 shows the effect of CyM treatment between days 15 and 28 in a 28 d BLM-induced lung fibrosis model. Online supplemental material is available at http://www.jem.org/cgi/content/full/jem.20101457/DC1.

We thank Drs. H.R. Kim and E. Choi for critical comments on the manuscript.

This work was supported by grants from MarineBio Technology Project, Ministry of Land, Transport, and Maritime Affairs (D-S. Lee) and Korea Healthcare Technology R&D Project, Ministry for Health, Welfare & Family Affairs (D-S. Lee; nos. A10019010110000100 and A08402210210000400).

The authors have declared that no conflict of interest exists.

Author contributions: K. Oh conducted most of the experiments. H.B. Park and O.J. Byoun performed the chimera study. D.M. Shin and E.M. Jeong performed some biochemical experiments in the supplemental data. Y.W. Kim, Y.S. Kim, and G. Melino interpreted the experimental results. D.S. Lee and K. Oh planned experimental approaches and analyzed and interpreted the experimental results. D.S. Lee, K. Oh, and I.G. Kim directed the project and wrote the paper.

Submitted: 20 July 2010
Accepted: 9 June 2011

REFERENCES

Akimov, S.S., and A.M. Belkin. 2001. Cell-surface transglutaminase promotes fibronectin assembly via interaction with the gelatin-binding domain of fibronectin: a role in TGFbeta-dependent matrix deposition. *J. Cell Sci.* 114:2989–3000.

Aujla, S.J., P.J. Dubin, and J.K. Kolls. 2007. Interleukin-17 in pulmonary host defense. *Exp. Lung Res.* 33:507–518. doi:10.1080/01902140701756604

Boisvert, W.A., D.M. Rose, A. Boullier, O. Quehenberger, A. Sydlaske, K.A. Johnson, L.K. Curtiss, and R. Terkeltaub. 2006. Leukocyte transglutaminase 2 expression limits atherosclerotic lesion size. *Arterioscler. Thromb. Vasc. Biol.* 26:563–569. doi:10.1161/01.ATV.0000203503.82693.c1

Braun, R.K., C. Ferrick, P. Neubauer, M. Sjoding, A. Sterner-Kock, M. Kock, L. Putney, D.A. Ferrick, D.M. Hyde, and R.B. Love. 2008. IL-17 producing gammadelta T cells are required for a controlled inflammatory response after bleomycin-induced lung injury. *Inflammation*. 31:167–179. doi:10.1007/s10753-008-9062-6

Chen, E.S., B.M. Greenlee, M. Wills-Karp, and D.R. Moller. 2001. Attenuation of lung inflammation and fibrosis in interferon-gamma-deficient mice after intratracheal bleomycin. *Am. J. Respir. Cell Mol. Biol.* 24:545–555.

Chua, F., S.E. Dunsmore, P.H. Clingen, S.E. Mutsaers, S.D. Shapiro, A.W. Segal, J. Roes, and G.J. Laurent. 2007. Mice lacking neutrophil elastase are resistant to bleomycin-induced pulmonary fibrosis. *Am. J. Pathol.* 170:65–74. doi:10.2353/ajpath.2007.060352

Cose, S., C. Brammer, K.M. Khanna, D. Masopust, and L. Lefrançois. 2006. Evidence that a significant number of naive T cells enter non-lymphoid organs as part of a normal migratory pathway. *Eur. J. Immunol.* 36:1423–1433. doi:10.1002/eji.200535539

Dailey, M.O. 1998. Expression of T lymphocyte adhesion molecules: regulation during antigen-induced T cell activation and differentiation. *Crit. Rev. Immunol.* 18:153–184.

De Laurenzi, V., and G. Melino. 2001. Gene disruption of tissue transglutaminase. *Mol. Cell. Biol.* 21:148–155. doi:10.1128/MCB.21.1.148-155.2001

Di Cesare, A., P. Di Meglio, and F.O. Nestle. 2009. The IL-23/Th17 axis in the immunopathogenesis of psoriasis. *J. Invest. Dermatol.* 129:1339–1350. doi:10.1038/jid.2009.59

du Bois, R.M. 2010. Strategies for treating idiopathic pulmonary fibrosis. *Nat. Rev. Drug Discov.* 9:129–140. doi:10.1038/nrd2958

Elli, L., C.M. Bergamini, M.T. Bardella, and D. Schuppan. 2009. Transglutaminases in inflammation and fibrosis of the gastrointestinal tract and the liver. *Dig. Liver Dis.* 41:541–550. doi:10.1016/j.dld.2008.12.095

Falasca, L., M.G. Farrace, A. Rinaldi, L. Tuosto, G. Melino, and M. Piacentini. 2008. Transglutaminase type II is involved in the pathogenesis of endotoxic shock. *J. Immunol.* 180:2616–2624.

Gaudry, C.A., E. Verderio, D. Aeschlimann, A. Cox, C. Smith, and M. Griffin. 1999. Cell surface localization of tissue transglutaminase is dependent on a fibronectin-binding site in its N-terminal beta-sandwich domain. *J. Biol. Chem.* 274:30707–30714. doi:10.1074/jbc.274.43.30707

Hardie, W.D., S.W. Glasser, and J.S. Hagood. 2009. Emerging concepts in the pathogenesis of lung fibrosis. *Am. J. Pathol.* 175:3–16. doi:10.2353/ajpath.2009.081170

Ientile, R., D. Caccamo, and M. Griffin. 2007. Tissue transglutaminase and the stress response. *Amino Acids*. 33:385–394. doi:10.1007/s00726-007-0517-0

Ivanov, I.I., L. Zhou, and D.R. Littman. 2007. Transcriptional regulation of Th17 cell differentiation. *Semin. Immunol.* 19:409–417. doi:10.1016/j.smim.2007.10.011

Johnson, T.S., M. Griffin, G.L. Thomas, J. Skill, A. Cox, B. Yang, B. Nicholas, P.J. Birckbichler, C. Muchaneta-Kubara, and A. Meguid El Nahas. 1997. The role of transglutaminase in the rat subtotal nephrectomy model of renal fibrosis. *J. Clin. Invest.* 99:2950–2960. doi:10.1172/JCI119490

Jones, H.A., J.B. Schofield, T. Krausz, A.R. Boobis, and C. Haslett. 1998. Pulmonary fibrosis correlates with duration of tissue neutrophil activation. *Am. J. Respir. Crit. Care Med.* 158:620–628.

Kebir, H., K. Kreymborg, I. Ifergan, A. Dodelet-Devillers, R. Cayrol, M. Bernard, F. Giuliani, N. Arbour, B. Becher, and A. Prat. 2007. Human TH17 lymphocytes promote blood-brain barrier disruption and central nervous system inflammation. *Nat. Med.* 13:1173–1175. doi:10.1038/nm1651

Kim, S.Y. 2006. Transglutaminase 2 in inflammation. *Front. Biosci.* 11:3026–3035. doi:10.2741/2030

Kim, R., and K.C. Meyer. 2008. Therapies for interstitial lung disease: past, present and future. *Ther. Adv. Respir. Dis.* 2:319–338. doi:10.1177/1753465808096948

Kojima, S., K. Nara, and D.B. Rifkin. 1993. Requirement for transglutaminase in the activation of latent transforming growth factor-beta in bovine endothelial cells. *J. Cell Biol.* 121:439–448. doi:10.1083/jcb.121.2.439

Korn, T., E. Bettelli, M. Oukka, and V.K. Kuchroo. 2009. IL-17 and Th17 Cells. *Annu. Rev. Immunol.* 27:485–517. doi:10.1146/annurev.immunol.021908.132710

Kuestner, R.E., D.W. Taft, A. Haran, C.S. Brandt, T. Brender, K. Lum, B. Harder, S. Okada, C.D. Ostrander, J.L. Kreindler, et al. 2007. Identification of the IL-17 receptor related molecule IL-17RC as the receptor for IL-17F. *J. Immunol.* 179:5462–5473.

Lee, D.S., C. Ahn, B. Ernst, J. Sprent, and C.D. Surh. 1999. Thymic selection by a single MHC/peptide ligand: autoreactive T cells are low-affinity cells. *Immunity*. 10:83–92. doi:10.1016/S1074-7613(00)80009-6

Li, M.O., Y.Y. Wan, S. Sanjabi, A.K. Robertson, and R.A. Flavell. 2006. Transforming growth factor-beta regulation of immune responses. *Annu. Rev. Immunol.* 24:99–146. doi:10.1146/annurev.immunol.24.021605.090737

Lo Re, S., L. Dumoutier, I. Couillin, C. Van Vyve, Y. Yakoub, F. Uwambayinema, B. Marien, S. van den Brûle, J. Van Snick, C. Uyttenhove, et al. 2010. IL-17A-producing gammadelta T and Th17 lymphocytes mediate lung inflammation but not fibrosis in experimental silicosis. *J. Immunol.* 184:6367–6377. doi:10.4049/jimmunol.0900459

Lorand, L., and R.M. Graham. 2003. Transglutaminases: crosslinking enzymes with pleiotropic functions. *Nat. Rev. Mol. Cell Biol.* 4:140–156. doi:10.1038/nrm1014

Manzo, A., and C. Pitzalis. 2007. Lymphoid tissue reactions in rheumatoid arthritis. *Autoimmun. Rev.* 7:30–34. doi:10.1016/j.autrev.2007.03.006

McGeachy, M.J., and D.J. Cua. 2008. Th17 cell differentiation: the long and winding road. *Immunity*. 28:445–453. doi:10.1016/j.immuni.2008.03.001

Park, S.S., J.M. Kim, D.S. Kim, I.H. Kim, and S.Y. Kim. 2006. Transglutaminase 2 mediates polymer formation of I-kappaBalpha through C-terminal glutamine cluster. *J. Biol. Chem.* 281:34965–34972. doi:10.1074/jbc.M604150200

Rogliani, P., M. Mura, M. Assunta Porretta, and C. Saltini. 2008. New perspectives in the treatment of idiopathic pulmonary fibrosis. *Ther. Adv. Respir. Dis.* 2:75–93. doi:10.1177/1753465808089363

Schnyder-Candrian, S., D. Togbe, I. Couillin, I. Mercier, F. Brombacher, V. Quesniaux, F. Fossiez, B. Ryffel, and B. Schnyder. 2006. Interleukin-17 is a negative regulator of established allergic asthma. *J. Exp. Med.* 203:2715–2725. doi:10.1084/jem.20061401

Serhan, C.N., and J. Savill. 2005. Resolution of inflammation: the beginning programs the end. *Nat. Immunol.* 6:1191–1197. doi:10.1038/ni1276

Shweke, N., N. Boulos, C. Jouanneau, S. Vandermeersch, G. Melino, J.C. Dussaule, C. Chatziantoniou, P. Ronco, and J.J. Boffa. 2008. Tissue transglutaminase contributes to interstitial renal fibrosis by favoring accumulation of fibrillar collagen through TGF-beta activation and cell infiltration. *Am. J. Pathol.* 173:631–642. doi:10.2353/ajpath.2008.080025

Sonnenberg, G.F., M.G. Nair, T.J. Kirn, C. Zaph, L.A. Fouser, and D. Artis. 2010. Pathological versus protective functions of IL-22 in airway inflammation are regulated by IL-17A. *J. Exp. Med.* 207:1293–1305. doi:10.1084/jem.20092054

Staton, T.L., A. Habtezion, M.M. Winslow, T. Sato, P.E. Love, and E.C. Butcher. 2006. CD8+ recent thymic emigrants home to and efficiently repopulate the small intestine epithelium. *Nat. Immunol.* 7:482–488. doi:10.1038/ni1319

Surh, C.D., D.S. Lee, W.P. Fung-Leung, L. Karlsson, and J. Sprent. 1997. Thymic selection by a single MHC/peptide ligand produces a semidiverse repertoire of CD4+ T cells. *Immunity*. 7:209–219. doi:10.1016/S1074-7613(00)80524-5

Thompson, E.D., H.L. Enriquez, Y.X. Fu, and V.H. Engelhard. 2010. Tumor masses support naive T cell infiltration, activation, and differentiation into effectors. *J. Exp. Med.* 207:1791–1804. doi:10.1084/jem.20092454

Traves, S.L., and L.E. Donnelly. 2008. Th17 cells in airway diseases. *Curr. Mol. Med.* 8:416–426. doi:10.2174/156652408785160998

Verderio, E.A., T. Johnson, and M. Griffin. 2004. Tissue transglutaminase in normal and abnormal wound healing: review article. *Amino Acids*. 26:387–404. doi:10.1007/s00726-004-0094-4

Weaver, C.T., R.D. Hatton, P.R. Mangan, and L.E. Harrington. 2007. IL-17 family cytokines and the expanding diversity of effector T cell lineages. *Annu. Rev. Immunol.* 25:821–852. doi:10.1146/annurev.immunol.25.022106.141557

Wilson, M.S., S.K. Madala, T.R. Ramalingam, B.R. Gochuico, I.O. Rosas, A.W. Cheever, and T.A. Wynn. 2010. Bleomycin and IL-1beta-mediated pulmonary fibrosis is IL-17A dependent. *J. Exp. Med.* 207:535–552. doi:10.1084/jem.20092121

Worbs, T., U. Bode, S. Yan, M.W. Hoffmann, G. Hintzen, G. Bernhardt, R. Förster, and O. Pabst. 2006. Oral tolerance originates in the intestinal immune system and relies on antigen carriage by dendritic cells. *J. Exp. Med.* 203:519–527. doi:10.1084/jem.20052016

Wynn, T.A. 2007. Common and unique mechanisms regulate fibrosis in various fibroproliferative diseases. *J. Clin. Invest.* 117:524–529. doi:10.1172/JCI31487